Reprint

NO.51

CI/SFB (M38)

UDC 53.082.6

MEASUREMENT ERRORS WITH SURFACE-MOUNTED HEAT FLUX SENSORS

H. Trethowen

Reprinted from ***BUILDING AND ENVIROMENT***
Vol.21, No.1 (1986)

BUILDING RESEARCH ASSOCIATION OF NEW ZEALAND

Building and Environment, Vol. 21, No. 1, pp. 41–56, 1986
Printed in Great Britain.

0360–1323/86 $3.00 + 0.00
Pergamon Journals Ltd.

Measurement Errors with Surface-mounted Heat Flux Sensors

H. TRETHOWEN*

Surface-mounted heat flux sensors (HFSs) have been increasingly used for measuring thermal performance in buildings. These measurements are inherently subject to some error, but the size and sources of these errors has been uncertain. This paper offers comprehensive, quantitative predictions of the magnitudes of the errors and of their relative influences. It concludes that there are three (predictable) regimes in which such HFSs may operate, each having very different sensitivities to particular physical environmental factors. There are some unexpected consequences in how these devices should be selected and used, particularly that large sensors have both accuracy and stability advantages, and that sensitivity to surface heat transfer coefficient depends on the operating regime, being most acute with small, low-resistance sensors.

1. INTRODUCTION

HEAT flux sensors (HFSs) were suggested by Houghten and Wood [1] in 1921, and have been used at least since 1924 when Nicholls [2] described their use. In essence, HFSs are formed from a wafer of some material across which a temperature difference is measured. Except during transients, the temperature difference so measured must be a function, usually a linear function, of the heat flux.

Unfortunately, because a temperature drop must exist, HFS devices must always be subject to some error and a disturbance to the heat flow conditions is inevitable. In practice this error can be made quite small, but normally with reduced sensitivity, and often reduced robustness and response time as well. The literature is rich in advice on what to do, but there is a lack of quantitative information on the importance of the various error sources. This paper aims to reverse this so that HFS devices can be optimised for the wide variety of task that they are used for.

This paper considers only surface-mounted sensors, with and without edge guards, and offers methods for predicting and avoiding measurement errors. These lead to some unexpected conclusions concerning selection and use of such sensors.

2. SCOPE

This paper addresses the measurement error of surface-mounted HFS devices for building heat flows under various physical and operating conditions. It attempts to do this largely by use of dimensionless parameters, based on finite-difference computer predictions. The correlation so obtained is then compared with previously reported measured errors and with an independent analytical solution.

The measurement errors the paper seeks to explain are those attributable to the presence of a sensor—the sensor itself is assumed throughout to be perfectly calibrated. The effects of various surface heat transfer coefficients are allowed for, but the heat transfer coefficients themselves are not examined.

Only steady-state conditions are considered here. This is partly to avoid undue complication, but for many purposes it may be sufficient. If dynamic measurements are needed, response can be approximated in one dimension.

The characteristics of heat flow around a HFS are illustrated in Fig. 1. There are two interacting systems, one system being the distribution of heat flows within the structure being measured, the other system being the surface heat transfer conditions around and over the sensor. The measurement error is seen as being made up of two parts, one being attributable to reduced heat flux where the sensor is located, the other part attributable to a portion of that reduced heat flux spilling around the edges of the sensor and thus not detected. The latter part is referred to below as 'edge spill'.

3. REVIEW OF LITERATURE

A substantial body of literature now exists on surface-mounted HFSs. This literature is reviewed below with respect to three specific topics: (a) calibration, (b) measurement errors, (c) sensitivity to lateral temperature difference. These are chosen simply because it is in these areas that the literature seems to be weakest.

The measurement errors considered here are largely those which are an unavoidable feature of the use of these devices. For this purpose all HFSs are considered to have been perfectly calibrated, i.e. their output is exactly interpretable to the corresponding mean flux of heat through the sensor. That heat flux will differ from the value which would have occurred in the absence of the sensor and calibration should aim to duplicate the same condition. Many references advocate the use of the guarded hotplate equipment for HFS calibration, but usually bypass the issue that (unless the guarded hotplate is built specifically for the HFS) there is a size difference between the HFS and guarded hotplate. The recommendation, of course, is to surround the HFS with a mask of 'similar material'.

This advice, though sound, raises the practical difficulty

* Building Research Association of New Zealand, BRANZ Private Bag, Porirua, New Zealand.

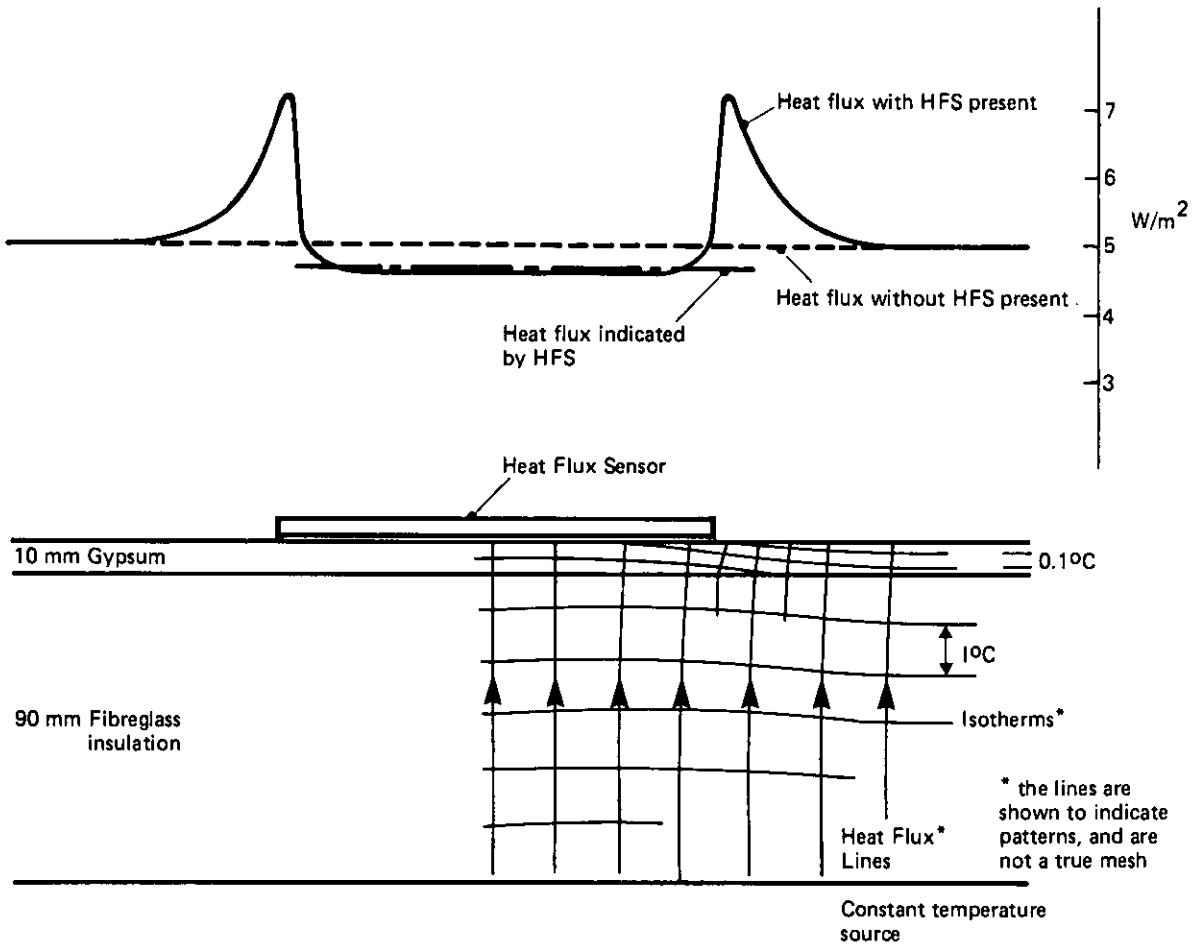

Fig. 1. Heat flow around a heat flux sensor, from finite-difference model.

that the thermal resistance of the sensor may not be known, or even if it is known, whether the thickness and resistance can be matched. It must be remembered that a high quality of match must be achieved if the guarded hotplate calibration is to be accurate. A second difficulty is that when surface mounted, HFSs lose heat from the edges as well as the face. The ratio of edge/face areas is disconcertingly large in some sensors. The guarded hotplate purposely excludes this factor. Calibrations by guarded hotplate may need to be adjusted for edge/face area ratio.

A final factor looked for in this review is sensitivity to lateral temperature gradients over the face of the sensor. If not avoided, signals from this source can easily swamp those due to normal heat flux.

Nicholls [2] described a series of sensors made from various materials. The dimensions were 600 mm (24 in.) square including a 110 mm ($4\frac{1}{2}$ in.) edge-guard area, 1–12 mm thick. Detection was by thermopile. An extensive discussion on calibration was provided, with calibration by a guarded hotplate apparatus. The guarded hotplate was built to accommodate samples of the size of the sensors. Either by accident or design (Nicholls does not mention the point) the wiring design gives a sensor not much affected by lateral temperature differences. In application of these sensors Nicholls [3] corrected for the series resistance of the sensor, but apparently had no way of estimating edge spill errors. Houghten *et al.* [4] used the same sensors, presumably with the same procedures.

Huebscher *et al.* [5] described a thermopile type of HFS constructed in quite a different way, in sizes 290 mm ($11\frac{1}{2}$ in.) and 400 mm (16 in.) square, 1.1 and 2.5 mm thick. Two procedures for relative or ranking calibration of a group of sensors were described. Guarded hotplate equipment was used for absolute calibration. However, in this case the size of HFS was not equal to the hotplate size, and some discussion is given on difficulties encountered in matching mask material with HFS for calibration. This was ultimately resolved only by going through a two-stage calibration process—first to rank order the sensors so that nearly matched sensors could be calibrated in pairs, with 6-mm hardboard packing and microcrystalline wax filling. In most cases no edge guarding was used.

The sensors were thin (1–2.5 mm) and had a very small thermal resistance (0.003 and 0.005 m^2 °C W^{-1}). Huebscher comments that the wiring sequence was chosen to minimise the effect of lateral temperature variations on sensor signal and is the only author discovered who has discussed this.

A considerable effort was made to show whether the calibration was stable. One sensor was cycled between an ice bath and an 85°C oven for 92 cycles, 15 min each. A 3.5% increase in output was observed after the first 18 cycles and no further change observed. Then 100 passes under a 20-kg

roller had no effect. A second sensor was cycled between −57°C (10 min) and 100°C (5 min) for 35 cycles, and again produced an increase in output of 3%. In application, the same correction for the series resistance of the sensor was used as by Nicholls, without attempt to account for edge spill.

Philip [6], and later Schwerdtfeger [7] carried out detailed analytic studies of HFSs and both are widely cited. However, these studies were directed solely at embedded sensors, and do not offer comment applicable to the surface-mounted case.

In 1962 De Jong and Marquenie [8] described the useful technique of producing many-junction thermopiles by electroplating. Calibration is stated to be by guarded hotplate but no details are given. No comment is given on either need or method to adjust indicated heat fluxes in use. It is worth nothing that in the coiled-coil form that this sensor type is wound, it will not be affected by lateral temperature gradients. This will not be true of the Schmidt and the Hencky sensors also mentioned in the paper, or of the linear forms of the De Jong and Marquenie sensors.

Johannesson [9] in 1976 presented quantitative data relating to the effect of local windspeed on measurement error, and also on the effect of thermal conductivity of the top substrate layer under the HFS. With respect to windspeed, he experimentally examined the effects of wind penetration under the sensor, concluding that air gaps less than 1 mm were not serious.

Heard and Ward [10] offered yet another sensor, using electroplated thermopile detectors. They achieve an excellent job of clarifying the sensor constructions used by earlier authors, whose own descriptions were somewhat obfuscatory. However, they did fall into a trap their predecessors largely avoided: their sensor would be badly affected by the presence of any lateral temperature gradients. Their application method was to embed their sensor within plasterboard and the calibration method they used was to duplicate this condition in a guarded hotplate.

Grot [11] in 1982 discussed surface-mounted HFSs in general, citing feasible overall accuracies within 6%. He recommended that only one method of calibration should be used—to sandwich the HFS in a 'similar' material, and then use the standard guarded hotplate technique. However, Grot does not discuss whether or how the indicated heat fluxes should be corrected when applying the sensors. Condon and Carroll [12] describe the application of HFSs in field measurements, with an aim of deducing the dynamic behaviour of the structure, but again do not discuss systematic measurement error.

Haupin and Luffy [13] described an extremely robust sensor, and introduced a completely new type of ring-guarded calibration hotplate. Because of the particular features of their procedures, they were able to show that for their HFS, the increase in heat flow attributable to extra surface at the sensor edges outweighed the decrease in heat flow attributable to the added resistance. However, the edge area in their case was 42% that of the face area, so this is not a surprising result. A fairly extensive correction function relating indicated to undisturbed heat flux is included. Regrettably this data is not resolvable into contributory parts, as essential information is not given, including the thermal resistance of the sensor, the emittance of sensor surface and guard plate, and/or the surface heat transfer coefficients. This means that Haupin and Luffy's data can not be compared with the predictive methods developed in this paper.

Flanders [14] in 1980 discussed in some detail the use of time-varying field heat flux and temperature data to derive *R*-values. He did not discuss HFS output correction, but noted that '. . . field . . . measurement techniques need improvement . . .' In 1982 [15, 16] he made further comment in the same vein. However in 1985 Flanders [17] discussed measurement errors directly and described a correction factor for a set of sensors, based on supplementary temperature difference information. He assessed the various sources of measurement error concluding that differences between the convective surface heat transfer coefficient over HFS and elsewhere were likely to be the dominant source of error for his conditions.

De Ponte and Maccato [18] discussed the possibility of errors due to inplane heat flows in HFS, although their discussion is confined to the calibration process in guarded hotplate and similar apparatus. They show that calibration errors from this source can readily exceed 1%, and point out hotplate design features to minimise such error.

Wright *et al.* [19] presented a description of laboratory attempts to account for errors due to sensor contact resistance with two types of commercial HFS. The stated resolution of temperature measuring equipment used (0.4 and 0.5 K) was barely adequate for the task, and represents worst-case uncertainties of 15–70% in derived heat fluxes. The reported discrepancies are greatest when the temperature differences are smallest, as is to be expected if measurement resolution is lacking. The paper shows that the thermal resistance of the sensors examined was small ($0.05\ m^2\ °C\ W^{-1}$), and that bonding agents are unreliable but excellent when they work.

Darnell *et al.* [20] in 1983 described another carefully conducted experimental series which carried out essentially two programmes. In one, they compared manufacturer's calibration data from two HFS suppliers with independent guarded hotplate tests, and noted differences of 17–44%. They also noted that the manufacturer's calibration often forecast the observed heat flows more closely than the independent one. Perhaps the manufacturers were aware that field results require adjustment and had anticipated it. In the second program the Darnell team mounted test 'panels' of single-layer material in a guarded hotbox pair and compared indicated and undisturbed heat fluxes. They used supplementary temperature measurements to assist in interpreting and correcting their indicated heat fluxes. However, their data is fairly complete and therefore valuable for testing any predictive model.

Trethowen [21] described the use of a heater-foil method of calibration which could cope with a wide range of HFS sizes. A preliminary attempt to correlate measurement errors by dimensionless parameters was also described.

To summarise the literature: over 20 papers dating from 1921 onward have been examined. In regard to calibration most have used the guarded hotplate and only two have used other methods. One author commented on 'considerable difficulty' in using the guarded hotplate with sensors of a non-matching size. No author has commented

on the effect of the edge/face area ratio of HFSs, although this ratio ranges from 1% or so to over 70%.

With regard to interpreting/correcting indicated heat fluxes, five authors have corrected for relative resistance only, three have attempted to correct for edge spill as well, and 13 make no comment at all. Experimental data against which predictive correction methods may be tested is very sparse, with only four authors offering data, and of these only two give sufficiently comprehensive data to permit comparison with the predictions presented here.

Only two authors have considered sensitivity to lateral temperature gradient worthy of comment, even though four of the sensors described have designs which avoid this problem, and six are almost certainly at risk of major errors if lateral temperature gradients are encountered.

4. PREDICTION OF MEASUREMENT ERROR

This paper develops a suggestion by Trethowen [21], for the quantitative prediction of measurement errors with surface-mounted HFSs. The term 'measurement error' is used here to refer to the difference between the heat flux which passes through the sensor and the heat flux which would have existed in the absence of any sensor.

Two methods are given here. The first is a dimensionless parametric method, empirically fitted to computer simulations. The second is an analytical method due to Weir [22]. Previously reported experimental data is then compared with the dimensionless parametric model.

The computer simulations for the parametric model have been obtained from two independent programs. Most (173 cases) were derived from a finite-difference program (HFSIM) written specifically for this situation, and described by Trethowen [21]. HFSIM can handle either two or three dimensions. A further 33 cases were derived using a DECUS finite-element program HEAT, which handles two dimensions only. The details of these simulations are listed in Tables 1 and 2.

From the data in Tables 1 and 2, the predicted measurement error was correlated empirically. First, multiple regression showed the relative influence of the physical variables. These variables were then forced into dimensionless groups, with the results shown in Fig. 2 and equations (1).

Firm top and bottom limits to the measurement error can be simply derived, corresponding to effectively zero and effectively infinite edge spill, respectively. If there is no edge spill (e.g. edge guards are present) then the error E must obviously have the value in equation (1a). On the other hand, if lateral heat flow is unimpeded, and the substrate is therefore isothermal, then equally clearly the error must have the value in equation (1b)

$$E = s \cdot cH^n \tag{1}$$

subject to:

$$E_{min} = R_m/(R_m + R_t) \tag{1a}$$

$$E_{max} = R_m/(R_m + R_s) \tag{1b}$$

$$H = \frac{R_m \cdot R_m}{R_t \cdot R_s} \sqrt{\frac{k \cdot t \cdot R_s}{L^2}} \tag{1c}$$

$$R_m = (R'_m + R_{ms} - R_s) \tag{1d}$$

where

$E = 1 - Q_i/Q_0$
Q_i = indicated heat flux
Q_0 = undisturbed heat flux
$s = \text{sgn}(R_m) (= \pm 1$, according to the sign of $R_m)$
c = fitted constant = 2.1136
n = fitted constant = 0.465
R'_m = HFS series resistance (including contact resistance)
R_{ms} = surface resistance over HFS
R_s = surface resistance over undisturbed structure
R_t = total thermal resistance of test structure
k = thermal conductivity of top substrate layer
t = thickness of top substrate layer
L = length or breadth of square HFS
$= 2AB/(A+B)$ for rectangular HFS
(this hydraulic radius formula diverges a little for very small sensors).

In Tables 1 and 2

t_i = thickness of insulation layer
k_i = conductivity of insulation layer
t_g = thickness of surface layer $(=t)$
k_g = conductivity of surface layer $(=k)$
R_z = thermal resistance (usually zero) between insulation and constant temperature source (see Fig. 1).

The characteristics of equation (1) are illustrated in Fig. 2, which forms the key part of this paper. It should be noted that there are three zones in Fig. 2, these will be discussed further. These will be referred to as follows:

—the 'power-law regime', described by equation (1)
—the 'insulation-controlled regime', described by equation (1a)
—the 'surface-controlled regime', described by equation (1b)

If H_{max} and H_{min} are the values of H corresponding to E_{min} and E_{max}, respectively, then the pattern in Fig. 2 can be normalised as in Fig. 3.

4.1. *Example*

As an example, consider the sensor used by Darnell *et al.* [20] over 50-mm expanded polystyrene board. Reconstructing from the paper we find (assuming no edge guarding is included):

Sensor size	L	= 0.05 m
Sensor + contact resistance	R'_m	= 0.042 m² °C W⁻¹
Surface resistance	R_s	= 0.07 m² °C W⁻¹
Total sample resistance	R_t	= 1.50 m² °C W⁻¹
Conductivity of surface layer	k	= 0.037 W m⁻¹ °C⁻¹
Thickness of surface layer	t	= 0.01–0.05 m.

(This particular sample is homogenous, and one may consider either that the entire 50-mm sample is the surface layer, or that some arbitrary lesser part of it is called the surface layer. Two values have been considered in this example.)

Table 1. Details of cases used to develop Fig. 2 (from HFSIM, three-dimensional)

		Input data										Derived data					
Row	Case	R_m	A	B	t_i	k_i	t_g	k_g	R_s	R_c	R_z	Q_i	Q_o	E	H	E_{min}	E_{max}
1	12.0	0.100	0.50	0.50	0.09	0.0500	0.010	0.160	0.120	0.030	0	4.3631	4.9690	0.1219	0.0019393	0.0607	0.5200
2	19.0	0.100	0.50	0.50	0.09	0.0500	0.010	0.250	0.120	0.030	0	4.3482	5.0255	0.1348	0.0024516	0.0613	0.5200
3	20.0	0.100	0.50	0.50	0.09	0.0500	0.010	0.250	0.030	0.030	0	4.3905	5.2634	0.1658	0.0051354	0.0640	0.8125
4	20.5	0.100	0.50	0.50	0.09	0.0500	0.010	0.250	0.060	0.030	0	4.3957	5.1812	0.1516	0.0035748	0.0631	0.6842
5	21.0	0.100	0.50	0.50	0.09	0.0500	0.010	0.250	0.090	0.030	0	4.3697	5.1017	0.1435	0.0028741	0.0622	0.5909
6	26.0	0.050	0.50	0.50	0.09	0.0500	0.010	0.160	0.120	0.030	0	4.5777	4.9690	0.0787	0.0007344	0.0382	0.4000
7	27.0	0.020	0.50	0.50	0.09	0.0500	0.010	0.160	0.120	0.030	0	4.7147	4.9690	0.0512	0.0002869	0.0242	0.2941
8	28.0	0.020	0.50	0.50	0.09	0.0500	0.010	0.160	0.120	0.010	0	4.8577	5.0187	0.0321	0.0001043	0.0148	0.2000
9	29.0	0.100	0.50	0.50	0.09	0.0500	0.010	0.160	0.120	0.010	0	4.4728	5.0187	0.1088	0.0014024	0.0523	0.4783
10	30.0	0.100	0.30	0.30	0.09	0.0500	0.010	0.160	0.120	0.030	0	4.2134	4.9688	0.1520	0.0032322	0.0607	0.5200
11	31.0	0.100	0.10	0.10	0.09	0.0500	0.010	0.160	0.120	0.030	0	3.7390	4.9688	0.2475	0.0096966	0.0607	0.5200
12	32.0	0.100	0.20	0.20	0.09	0.0500	0.010	0.160	0.120	0.030	0	4.0441	4.9688	0.1861	0.0048483	0.0607	0.5200
13	33.0	0.100	0.50	0.50	0.09	0.1000	0.010	0.160	0.120	0.030	0	7.5082	8.9889	0.1647	0.0035082	0.1046	0.5200
14	34.0	0.100	0.50	0.50	0.09	0.2000	0.010	0.160	0.120	0.030	0	11.8267	15.0951	0.2165	0.0058912	0.1640	0.5200
15	35.0	0.100	0.50	0.50	0.09	0.0300	0.010	0.160	0.120	0.030	0	2.8148	3.1131	0.0958	0.0012149	0.0389	0.5200
16	36.0	0.100	0.50	0.50	0.09	0.0500	0.010	0.100	0.120	0.030	0	4.3419	4.8806	0.1104	0.0015051	0.0596	0.5200
17	38.0	0.100	0.20	0.20	0.09	0.2000	0.010	0.160	0.120	0.030	0	11.0416	15.0942	0.2685	0.0147279	0.1640	0.5200
18	39.0	0.050	0.50	0.50	0.09	0.2000	0.010	0.160	0.120	0.030	0	12.9026	15.0951	0.1452	0.0022310	0.1077	0.4000
19	41.0	0.100	0.50	0.50	0.09	0.2000	0.010	0.300	0.120	0.030	0	11.9493	15.4877	0.2285	0.0084383	0.1703	0.5200
20	42.0	0.100	0.50	0.50	0.09	0.2000	0.010	0.200	0.120	0.030	0	11.9444	15.3855	0.2237	0.0067132	0.1667	0.5200
21	43.0	0.100	0.50	0.50	0.09	0.2000	0.010	0.100	0.120	0.030	0	11.4391	14.2867	0.1993	0.0044079	0.1566	0.5200
22	44.0	0.100	0.50	0.50	0.09	0.2000	0.010	0.050	0.120	0.030	0	10.3763	12.4999	0.1699	0.0027272	0.1398	0.5200
23	48.0	0.100	0.50	0.50	0.09	0.2000	0.010	0.160	0.170	0.030	0	11.3076	14.0702	0.1963	0.0046022	0.1543	0.4333
24	49.0	0.100	0.50	0.50	0.09	0.2000	0.010	0.160	0.050	0.030	0	12.9651	17.1865	0.2456	0.0102048	0.1799	0.7222
25	50.0	0.100	0.50	0.50	0.09	0.0500	0.010	0.050	0.120	0.030	0	4.2229	4.6513	0.0921	0.0010148	0.0570	0.5200
26	52.0	0.100	0.20	0.20	0.09	0.1600	0.010	1.300	0.120	0.030	0	8.9722	13.8851	0.3538	0.0386180	0.1529	0.5200
27	53.0	0.100	0.20	0.20	0.09	0.0500	0.010	0.300	0.120	0.030	0	3.9478	5.0427	0.2171	0.0067364	0.0615	0.5200
28	54.0	0.100	0.20	0.20	0.09	1.0000	0.010	0.500	0.120	0.030	0	23.2595	38.5524	0.3967	0.0663404	0.3333	0.5200
29	56.0	0.020	0.20	0.20	0.09	1.0000	0.010	0.500	0.120	0.010	0	35.8186	41.7043	0.1411	0.0038273	0.1111	0.2000
30	57.0	0.010	0.50	0.50	0.09	0.0500	0.010	0.160	0.150	0.005	0	4.8745	4.9565	0.0165	0.0000230	0.0074	0.0909
31	58.0	0.020	0.20	0.20	0.09	1.0000	0.010	0.500	0.100	0.005	0	40.1918	46.5522	0.1366	0.0032501	0.1042	0.2000
32	59.0	0.020	0.20	0.20	0.09	1.0000	0.010	0.500	0.060	0.005	0	47.1423	57.2111	0.1760	0.0051549	0.1250	0.2941
33	60.0	0.020	0.20	0.20	0.09	1.0000	0.010	0.500	0.030	0.005	0	53.4675	69.0675	0.2259	0.0087985	0.1471	0.4545
34	61.0	0.100	0.50	0.50	0.09	0.0350	0.010	0.035	0.170	0.005	0	3.1037	3.2980	0.0589	0.0003300	0.0335	0.3818
35	62.0	0.100	0.50	0.50	0.09	0.0350	0.010	0.250	0.170	0.005	0	3.2520	3.5890	0.0939	0.0009596	0.0363	0.3818
36	63.0	0.100	0.50	0.50	0.09	0.0350	0.010	0.250	0.060	0.005	0	3.3136	3.7366	0.1132	0.0016817	0.0378	0.6364
37	65.0	0.010	0.50	0.50	0.09	0.5000	0.010	0.160	0.150	0.001	0	4.9068	4.9663	0.0120	0.0000124	0.0054	0.0683
38	66.0	0.020	0.50	0.50	0.09	0.0300	0.010	0.100	0.150	0.002	0	3.0157	3.0750	0.0193	0.0000243	0.0067	0.1279
39	67.0	0.100	0.50	0.50	0.09	0.0200	0.010	0.160	0.150	0.010	0	1.9609	2.1177	0.0740	0.0005292	0.0228	0.4231
40	68.0	0.100	0.50	0.50	0.09	0.0350	0.010	0.035	0.150	0.010	0	3.1166	3.3143	0.0597	0.0003874	0.0352	0.4231
41	71.0	0.100	0.20	0.50	0.09	0.0500	0.010	0.160	0.120	0.030	0	4.1839	4.9691	0.1580	0.0033938	0.0607	0.5200
42	72.0	0.100	0.10	0.50	0.09	0.0500	0.010	0.160	0.120	0.030	0	3.9859	4.9691	0.1979	0.0058180	0.0607	0.5200

Table 1 (*continued*)

		Input data										Derived data					
Row	Case	R_m	A	B	t_i	k_i	t_g	k_g	R_s	R_c	R_z	Q_i	Q_o	E	H	E_{min}	E_{max}
43	73.0	0.100	0.30	0.50	0.09	0.0500	0.010	0.160	0.120	0.030	0	4.2818	4.9691	0.1383	0.0025858	0.0607	0.5200
44	74.0	0.100	0.40	0.50	0.09	0.0500	0.010	0.160	0.120	0.030	0	4.3377	4.9690	0.1270	0.0021817	0.0607	0.5200
45	75.0	0.100	0.20	0.20	0.09	0.0500	0.010	0.160	0.120	0.030	0	4.0383	4.9688	0.1873	0.0048483	0.0607	0.5200
46	77.0	0.100	0.16	0.20	0.09	0.0500	0.010	0.160	0.120	0.030	0	4.0024	4.9688	0.1945	0.0054543	0.0607	0.5200
47	78.0	0.100	0.10	0.20	0.09	0.0500	0.010	0.160	0.120	0.030	0	3.8679	4.9688	0.2216	0.0072725	0.0607	0.5200
48	79.0	0.100	0.06	0.20	0.09	0.0500	0.010	0.160	0.120	0.030	0	3.5938	4.9688	0.2767	0.0105047	0.0607	0.5200
49	80.0	0.100	0.04	0.20	0.09	0.0500	0.010	0.160	0.120	0.030	0	3.5304	4.9688	0.2895	0.0145449	0.0607	0.5200
50	81.0	0.100	0.02	0.02	0.09	0.0500	0.010	0.160	0.120	0.030	0	3.2340	4.9688	0.3491	0.0266657	0.0607	0.5200
51	82.0	0.100	0.02	0.02	0.09	0.0500	0.010	0.160	0.120	0.030	0	2.9922	4.9688	0.3978	0.0484831	0.0607	0.5200
52	83.0	0.100	0.02	0.04	0.09	0.0500	0.010	0.160	0.120	0.030	0	3.0969	4.9688	0.3767	0.0363623	0.0607	0.5200
53	84.0	0.100	0.04	0.04	0.09	0.0500	0.010	0.160	0.120	0.030	0	3.2781	4.9688	0.3403	0.0242415	0.0607	0.5200
54	85.0	0.100	0.10	0.10	0.09	0.0500	0.010	0.160	0.120	0.030	0	3.7388	4.9688	0.2475	0.0096966	0.0607	0.5200
55	86.0	0.100	0.04	0.50	0.09	0.0500	0.010	0.160	0.120	0.030	0	3.5938	4.9688	0.2767	0.0130904	0.0607	0.5200
56	87.0	0.100	0.08	0.50	0.09	0.0500	0.010	0.160	0.120	0.030	0	3.3000	4.9692	0.3359	0.0070300	0.0607	0.5200
57	88.0	0.100	0.08	0.10	0.09	0.0500	0.010	0.160	0.120	0.030	0	3.6588	4.9692	0.2637	0.0109087	0.0607	0.5200
58	89.0	0.100	0.06	0.10	0.09	0.0500	0.010	0.160	0.120	0.030	0	3.5810	4.9692	0.2794	0.0129288	0.0607	0.5200
59	90.0	0.100	0.04	0.10	0.09	0.0500	0.010	0.160	0.120	0.030	0	3.4615	4.9692	0.3034	0.0169691	0.0607	0.5200
60	91.0	0.100	0.02	0.10	0.09	0.0500	0.010	0.160	0.120	0.030	0	3.1939	4.9692	0.3573	0.0290898	0.0607	0.5200
61	92.0	0.100	0.30	0.30	0.09	0.0500	0.010	0.160	0.120	0.030	0	4.2162	4.9690	0.1515	0.0032322	0.0607	0.5200
62	93.0	0.100	0.40	0.40	0.09	0.0500	0.010	0.160	0.120	0.030	0	4.3191	4.9691	0.1308	0.0024242	0.0607	0.5200
63	94.0	0.100	0.36	0.40	0.09	0.0500	0.010	0.160	0.120	0.030	0	4.2300	4.9691	0.1487	0.0025588	0.0607	0.5200
64	102.0	0.100	0.50	0.50	0.09	0.0500	0.005	0.320	0.120	0.030	0	4.4227	5.0878	0.1307	0.0019856	0.0620	0.5200
65	103.0	0.100	0.50	0.50	0.09	0.0500	0.005	0.160	0.120	0.030	0	4.4569	5.0472	0.1170	0.0013929	0.0616	0.5200
66	104.0	0.100	0.50	0.50	0.09	0.0500	0.020	0.160	0.120	0.030	0	4.2142	4.8156	0.1249	0.0026600	0.0590	0.5200
67	105.0	0.100	0.50	0.50	0.06	0.0500	0.010	0.160	0.120	0.030	0	6.0766	7.0795	0.1417	0.0027631	0.0843	0.5200
68	107.0	0.030	0.10	0.10	0.09	0.0500	0.010	0.160	0.120	0.030	0	4.3164	4.9688	0.1313	0.0020656	0.0290	0.3333
69	108.0	0.010	0.10	0.10	0.09	0.0500	0.010	0.160	0.120	0.010	0	4.7694	5.0187	0.0497	0.0002318	0.0099	0.1429
70	109.0	0.100	100.00	100.00	0.09	0.0500	0.010	0.160	0.120	0.010	0	4.7683	5.0188	0.0499	0.0000070	0.0523	0.4783
71	110.0	0.100	0.50	0.50	0.09	0.0500	0.010	0.050	0.120	0.030	0	4.2210	4.6512	0.0925	0.0010148	0.0570	0.5200
72	111.0	0.100	0.50	0.50	0.09	0.0350	0.010	0.035	0.120	0.030	0	3.0954	3.3255	0.0692	0.0006070	0.0414	0.5200
73	114.0	0.100	0.50	0.50	0.09	1.3000	0.010	1.300	0.120	0.030	0	26.2100	44.4300	0.4101	0.0490252	0.3642	0.5200

74	116.0	0.100	100.00	0.04	0.09	0.0500	0.010	0.170	0.250	0.030	0	3.7200	4.6756	0.2044	0.0081480	0.0573	0.3421
75	117.0	0.030	0.50	0.50	0.09	0.1000	0.010	0.160	0.120	0.010	0	8.6095	9.1533	0.0594	0.0003382	0.0353	0.2500
76	118.0	0.030	0.30	0.30	0.09	0.1000	0.010	0.160	0.120	0.010	0	8.5000	9.1533	0.0714	0.0005637	0.0353	0.2500
77	119.0	0.030	0.20	0.20	0.09	0.1000	0.010	0.160	0.120	0.010	0	8.3650	9.1540	0.0862	0.0008455	0.0353	0.2500
78	120.0	0.030	0.10	0.10	0.09	0.1000	0.010	0.160	0.120	0.010	0	8.1600	9.1500	0.1082	0.0016911	0.0353	0.2500
79	121.0	0.030	0.06	0.06	0.09	0.1000	0.010	0.160	0.120	0.010	0	7.9440	9.1540	0.1322	0.0028185	0.0353	0.2500
80	122.0	0.030	0.02	0.02	0.09	0.1000	0.010	0.160	0.120	0.010	0	7.5620	9.1540	0.1739	0.0084555	0.0353	0.2500
81	123.0	0.030	0.50	0.50	0.09	0.1364	0.010	0.160	0.360	0.010	0	8.7130	9.1550	0.0483	0.0001953	0.0353	0.1000
82	124.0	0.030	0.50	0.50	0.09	0.0580	0.010	0.160	0.360	0.030	0	4.7500	4.9900	0.0481	0.0002395	0.0291	0.1429
83	125.0	0.030	0.50	0.50	0.09	0.0500	0.010	0.160	0.120	0.010	0	4.8080	5.0190	0.0420	0.0001854	0.0197	0.2500
84	126.0	0.030	0.30	0.30	0.09	0.0500	0.010	0.160	0.120	0.010	0	4.7380	5.0190	0.0560	0.0003091	0.0197	0.2500
85	127.0	0.030	0.20	0.20	0.09	0.0500	0.010	0.160	0.120	0.010	0	4.6720	5.0190	0.0691	0.0004636	0.0197	0.2500
86	128.0	0.030	0.10	0.10	0.09	0.0500	0.010	0.160	0.120	0.010	0	4.5440	5.0190	0.0946	0.0009272	0.0197	0.2500
87	129.0	0.030	0.04	0.04	0.09	0.0500	0.010	0.160	0.120	0.010	0	4.3240	5.0190	0.1385	0.0023181	0.0197	0.2500
88	130.0	0.030	0.20	0.02	0.09	0.0500	0.010	0.160	0.120	0.010	0	4.1650	5.0190	0.1702	0.0046362	0.0197	0.2500
89	131.0	0.030	0.50	0.50	0.09	0.0580	0.010	0.160	0.360	0.010	0	4.8660	5.0400	0.0345	0.0001075	0.0198	0.1000
90	132.0	0.015	0.50	0.50	0.09	0.0253	0.010	0.160	0.360	0.005	0	2.4800	2.5100	0.0120	0.0000134	0.0050	0.0526
91	133.0	0.015	0.50	0.50	0.09	0.1572	0.010	0.160	0.360	0.005	0	9.7480	10.0000	0.0252	0.0000533	0.0196	0.0526
92	134.0	0.015	0.04	0.04	0.09	0.0579	0.010	0.160	0.380	0.005	0	4.8130	4.9960	0.0366	0.0003241	0.0099	0.0500
93	135.0	0.015	0.02	0.02	0.09	0.0579	0.010	0.160	0.380	0.005	0	4.7870	4.9960	0.0418	0.0006483	0.0099	0.0500
94	136.0	0.015	0.04	0.04	0.09	0.0500	0.010	0.160	0.120	0.005	0	4.6590	5.0320	0.0741	0.0005810	0.0100	0.1429
95	137.0	0.015	0.02	0.02	0.09	0.0500	0.010	0.160	0.120	0.005	0	4.5660	5.0320	0.0926	0.0011620	0.0100	0.1429
96	138.0	0.015	0.04	0.04	0.09	0.0479	0.010	0.160	0.060	0.005	0	4.4930	4.9840	0.0985	0.0008139	0.0099	0.2500
97	139.0	0.015	0.02	0.02	0.09	0.0479	0.010	0.160	0.060	0.005	0	4.3300	4.9800	0.1305	0.0016278	0.0099	0.2500
98	140.0	0.015	0.04	0.04	0.09	0.0473	0.010	0.160	0.030	0.005	0	4.4020	5.0000	0.1196	0.0011546	0.0099	0.4000
99	141.0	0.015	0.02	0.02	0.09	0.0473	0.010	0.160	0.030	0.005	0	4.1720	5.0000	0.1656	0.0023091	0.0099	0.4000
100	142.0	0.100	0.50	0.50	0.09	0.0250	0.010	0.160	0.030	0.010	0	2.4320	2.7010	0.0996	0.0015095	0.0289	0.7857
101	143.0	0.100	0.30	0.30	0.09	0.0250	0.010	0.160	0.030	0.010	0	2.3320	2.7010	0.1366	0.0025158	0.0289	0.7857
102	144.0	0.100	0.10	0.10	0.09	0.0250	0.010	0.160	0.030	0.010	0	1.9760	2.7010	0.2684	0.0075473	0.0289	0.7857
103	145.0	0.100	0.04	0.04	0.09	0.0250	0.010	0.160	0.030	0.010	0	1.5700	2.7010	0.4187	0.0188682	0.0289	0.7857
104	146.0	0.100	0.02	0.02	0.09	0.0250	0.010	0.160	0.030	0.010	0	1.3080	2.7010	0.5157	0.0377363	0.0289	0.7857
105	147.0	0.100	0.50	0.50	0.09	0.0250	0.010	0.050	0.030	0.010	0	2.5300	2.7020	0.0637	0.0008136	0.0278	0.7857
106	148.0	0.050	0.50	0.50	0.09	0.0125	0.010	0.050	0.030	0.010	0	1.3110	1.3440	0.0246	0.0001249	0.0080	0.6667
107	148.5	0.050	0.30	0.30	0.09	0.0125	0.010	0.050	0.030	0.010	0	1.2990	1.3440	0.0335	0.0002082	0.0080	0.6667
108	150.0	0.050	0.50	0.50	0.09	0.0500	0.010	0.050	0.015	0.010	0	4.6820	4.9380	0.0518	0.0006492	0.0288	0.8000
109	151.0	0.050	0.50	0.50	0.09	0.0500	0.010	0.050	0.120	0.010	0	4.4790	4.6947	0.0459	0.0002182	0.0274	0.3333

Table 2. Details of cases used to develop Fig. 2 (from HFSIM, two-dimensional)

		Input data										Derived data					
Row	Case	R_m	A	B	t_i	k_i	t_g	k_g	R_s	R_c	R_z	Q_i	Q_o	E	H	E_{min}	E_{max}
1	201.0	0.100	0.26	1000	0.0900	0.0500	0.010	0.160	0.1200	0.030	0.000	4.4353	5.0481	0.1214	0.001865	0.0607	0.5200
2	202.0	0.015	0.50	1000	0.0900	0.0579	0.010	0.160	0.3800	0.005	0.000	4.9271	4.9957	0.0137	0.000013	0.0099	0.0500
3	203.0	0.015	0.30	1000	0.0900	0.0579	0.010	0.160	0.3800	0.005	0.000	4.9061	4.9957	0.0179	0.000022	0.0099	0.0500
4	204.0	0.015	0.10	1000	0.0900	0.0579	0.010	0.160	0.3800	0.005	0.000	4.8705	4.9957	0.0251	0.000065	0.0099	0.0500
5	205.0	0.015	0.02	1000	0.0900	0.0579	0.010	0.160	0.3800	0.005	0.000	4.8115	4.9957	0.0369	0.000324	0.0099	0.0500
6	206.0	0.015	0.50	1000	0.0900	0.0500	0.010	0.160	0.1200	0.005	0.000	4.9374	5.0456	0.0214	0.000023	0.0100	0.1429
7	207.0	0.015	0.30	1000	0.0900	0.0500	0.010	0.160	0.1200	0.005	0.000	4.9192	5.0456	0.0263	0.000039	0.0100	0.1429
8	208.0	0.015	0.10	1000	0.0900	0.0500	0.010	0.160	0.1200	0.005	0.000	4.8345	5.0456	0.0418	0.000116	0.0100	0.1429
9	209.0	0.015	0.06	1000	0.0900	0.0500	0.010	0.160	0.1200	0.005	0.000	4.7820	5.0456	0.0522	0.000194	0.0100	0.1429
10	210.0	0.015	0.02	1000	0.0900	0.0500	0.010	0.160	0.1200	0.005	0.000	4.6532	5.0456	0.0778	0.000581	0.0100	0.1429
11	210.5	0.015	0.02	1000	0.0900	0.0500	0.010	0.640	0.1200	0.005	0.000	4.6170	5.1542	0.1042	0.001190	0.0102	0.1429
12	211.0	0.015	0.02	1000	0.0900	0.0250	0.010	0.640	0.1200	0.005	0.000	2.4020	2.6763	0.1025	0.000617	0.0053	0.1429
13	212.0	0.015	0.02	1000	0.0900	1.0000	0.010	0.640	0.1200	0.005	0.000	38.0870	43.1160	0.1166	0.010014	0.0798	0.1429
14	213.0	0.015	0.02	1000	0.0900	0.4000	0.010	0.640	0.1200	0.005	0.000	24.1714	27.3940	0.1176	0.006316	0.0519	0.1429
15	214.0	0.015	0.02	1000	0.0900	0.1500	0.010	0.640	0.1200	0.005	0.000	12.0224	13.5220	0.1109	0.003118	0.0263	0.1429
16	215.0	0.015	1.00	1000	0.0900	0.0579	0.010	0.160	0.3800	0.005	0.000	4.9320	4.9982	0.0132	0.000006	0.0099	0.0500
17	216.0	0.015	1.00	1000	0.0900	0.0579	0.010	0.040	0.3800	0.005	0.000	4.5180	4.5695	0.0113	0.000003	0.0091	0.0500
18	217.0	0.015	1.00	1000	0.0900	0.0550	0.010	0.040	0.1200	0.005	0.000	4.9119	4.9745	0.0126	0.000006	0.0098	0.1429
19	218.0	0.010	0.26	1000	0.0900	0.0500	0.010	0.160	0.1500	0.005	0.000	4.8662	4.9594	0.0188	0.000022	0.0074	0.0909
20	219.0	0.100	0.26	1000	0.0900	0.0350	0.010	0.035	0.1700	0.005	0.000	3.0751	3.3050	0.0696	0.000317	0.0335	0.3818
21	220.0	0.100	0.26	1000	0.0900	0.0500	0.010	0.160	0.1200	0.030	0.000	4.2664	4.9833	0.1439	0.001865	0.0607	0.5200
22	222.0	0.100	0.26	1000	0.0450	0.0250	0.005	0.320	0.1200	0.030	0.000	4.4826	5.0879	0.1190	0.001910	0.0620	0.5200
23	223.0	0.100	0.26	1000	0.0450	0.0250	0.005	0.320	0.1200	0.030	0.047	4.3531	4.9691	0.1240	0.001865	0.0607	0.5200
24	225.0	0.100	0.26	1000	0.0900	0.0600	0.010	0.160	0.1200	0.030	0.300	4.3466	4.9693	0.1253	0.001865	0.0607	0.5200
25	228.0	0.100	0.26	1000	0.0900	0.1600	0.010	0.160	0.1200	0.030	0.000	10.3403	12.9037	0.1987	0.004844	0.1436	0.5200
26	229.0	0.100	0.26	1000	0.0800	0.1600	0.020	0.160	0.1200	0.030	0.000	10.4071	12.9035	0.1935	0.006850	0.1436	0.5200
27	229.5	0.100	0.26	1000	0.0950	0.1600	0.005	0.160	0.1200	0.030	0.000	10.3116	12.9046	0.2009	0.003425	0.1436	0.5200
28	230.0	0.010	0.26	1000	0.0225	0.0125	0.010	0.160	0.1200	0.001	0.000	4.9843	5.0417	0.0114	0.000014	0.0055	0.0840
29	231.0	0.010	0.26	1000	0.1800	0.1000	0.010	0.160	0.1200	0.001	0.000	4.9749	5.0419	0.0133	0.000014	0.0055	0.0840
30	232.0	0.100	0.26	1000	0.1800	0.1000	0.010	0.160	0.1200	0.001	0.000	4.3154	4.9730	0.1322	0.001142	0.0485	0.4570

31	233.0	0.100	0.26	1000	0.0225	0.0125	0.010	0.160	0.1200	0.001	0.000	4.3990	4.9671	0.1144	0.001142	0.0485	0.4570
32	234.0	0.100	0.50	1000	0.0900	0.0500	0.010	0.160	0.1200	0.030	0.000	4.5028	4.9710	0.0942	0.000970	0.0607	0.5200
33	235.0	0.100	0.26	1000	0.0900	0.0500	0.010	0.160	0.1200	0.030	0.000	4.3688	4.9692	0.1208	0.001865	0.0607	0.5200
34	236.0	0.100	0.26	1000	0.0450	0.0500	0.010	0.160	0.1200	0.030	0.000	7.5744	8.9889	0.1574	0.003374	0.1046	0.5200
35	237.0	0.100	0.26	1000	0.0150	0.0500	0.010	0.160	0.1200	0.030	0.000	14.8836	19.5121	0.2372	0.007324	0.2023	0.5200
36	238.0	0.100	0.26	1000	0.0150	0.0500	0.005	0.160	0.1200	0.030	0.000	15.6021	20.7794	0.2492	0.005515	0.2127	0.5200
37	239.0	0.010	0.26	1000	0.0150	0.0500	0.005	0.160	0.1200	0.000	0.030	20.2204	20.7794	0.0269	0.000033	0.0204	0.0769
38	240.0	0.010	0.26	1000	0.0150	0.0500	0.002	0.160	0.1200	0.000	0.030	20.9854	21.6223	0.0295	0.000021	0.0212	0.0769
39	241.0	0.010	0.26	1000	0.0060	0.0500	0.002	0.160	0.1200	0.000	0.030	33.8874	35.3979	0.0427	0.000035	0.0342	0.0769
40	242.0	0.010	0.26	1000	0.0060	0.2500	0.002	0.400	0.1200	0.000	0.030	52.4591	55.8654	0.0610	0.000088	0.0529	0.0769
41	243.0	0.010	0.26	1000	0.0060	0.2500	0.002	0.400	0.1200	0.000	0.060	44.9694	47.8546	0.0603	0.000075	0.0457	0.0769
42	244.0	0.010	0.26	1000	0.0060	0.6000	0.002	0.600	0.1200	0.000	0.060	48.4731	51.6917	0.0623	0.000099	0.0492	0.0769
43	245.0	0.010	0.26	1000	0.0060	1.0000	0.002	1.000	0.1200	0.000	0.060	49.6393	53.1887	0.0667	0.000132	0.0505	0.0769
44	246.0	0.010	0.26	1000	0.0030	1.0000	0.001	1.000	0.1200	0.000	0.060	49.4750	54.4978	0.0922	0.000095	0.0515	0.0769
45	247.0	0.020	0.10	1000	0.0900	0.1400	0.010	0.340	0.3100	0.000	0.000	9.8232	10.1828	0.0353	0.000213	0.0200	0.0606
46	248.0	0.060	0.10	1000	0.0900	0.1300	0.010	1.670	0.2400	0.000	0.000	9.2565	10.7346	0.1377	0.005061	0.0601	0.2000
47	249.0	0.060	0.10	1000	0.0900	0.1300	0.010	1.670	0.1200	0.000	0.000	9.6990	12.2412	0.2077	0.008207	0.0683	0.3333
48	250.0	0.060	0.10	1000	0.0900	0.1300	0.010	1.670	0.0600	0.000	0.000	9.4640	13.1989	0.2830	0.012524	0.0733	0.5000
49	251.0	0.060	0.10	1000	0.0900	0.1300	0.010	1.670	0.0300	0.000	0.000	8.8109	13.7365	0.3586	0.018442	0.0761	0.6667
50	252.0	0.060	0.10	1000	0.0900	0.1300	0.010	1.670	0.0100	0.000	0.000	7.6488	14.1215	0.4584	0.032844	0.0781	0.8571
51	253.0	0.060	0.10	1000	0.0900	0.1300	0.010	1.670	0.0010	0.000	0.000	6.4158	14.3030	0.5514	0.105199	0.0790	0.9836
52	254.0	0.060	0.02	1000	0.0900	0.1300	0.010	1.670	0.0010	0.000	0.000	2.4179	14.3017	0.8309	0.525955	0.0790	0.9836
53	255.0	0.060	0.02	1000	0.0900	0.1300	0.010	1.670	0.0100	0.000	0.000	4.0711	14.1169	0.7116	0.164208	0.0781	0.8571
54	256.0	0.060	0.02	1000	0.0900	0.1300	0.010	1.670	0.0300	0.000	0.000	6.1336	13.7296	0.5533	0.092202	0.0761	0.6667
55	257.0	0.060	0.02	1000	0.0900	0.1300	0.010	1.670	0.0600	0.000	0.000	7.6278	13.1868	0.4216	0.062617	0.0733	0.5000
56	258.0	0.060	0.02	1000	0.0900	0.1300	0.010	1.670	0.1200	0.000	0.000	8.6817	12.2216	0.2896	0.041031	0.0683	0.3333
57	259.0	0.060	0.02	1000	0.0900	0.1300	0.010	1.670	0.2400	0.000	0.000	8.7361	10.6597	0.1805	0.025303	0.0601	0.2000
58	260.0	0.060	0.26	1000	0.0900	0.1300	0.010	1.670	0.2400	0.000	0.000	9.5087	10.8013	0.1197	0.001947	0.0601	0.2000
59	261.0	0.060	0.26	1000	0.0900	0.1300	0.010	1.670	0.1200	0.000	0.000	10.4061	12.3973	0.1606	0.003157	0.0683	0.3333
60	262.0	0.060	0.26	1000	0.0900	0.1300	0.010	1.670	0.0600	0.000	0.000	10.6565	13.3250	0.2003	0.004818	0.0733	0.5000
61	263.0	0.060	0.26	1000	0.0900	0.1300	0.010	1.670	0.0300	0.000	0.000	10.5060	13.8093	0.2392	0.007094	0.0761	0.6667
62	264.0	0.060	0.26	1000	0.0900	0.1300	0.010	1.670	0.0100	0.000	0.000	9.9647	14.1524	0.2959	0.012634	0.0781	0.8571
63	265.0	0.060	0.26	1000	0.0900	0.1300	0.010	1.670	0.0010	0.000	0.000	9.2103	14.3218	0.3569	0.040468	0.0790	0.9836
64	266.0	0.060	0.26	1000	0.0900	0.1300	0.010	1.670	0.0001	0.000	0.000	9.0772	14.3211	0.3662	0.128135	0.0791	0.9983

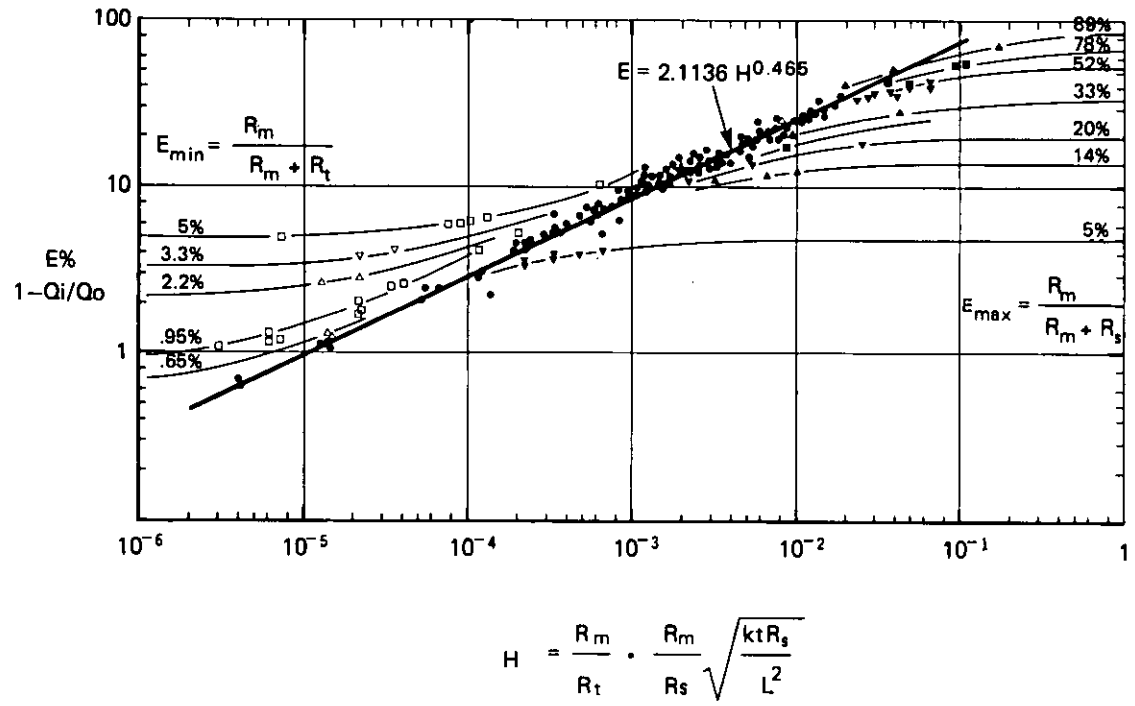

$$H = \frac{R_m}{R_t} \cdot \frac{R_m}{R_s}\sqrt{\frac{ktR_s}{L^2}}$$

Three operating regimes are defined :—

Power Law Regime — Comprising the points which fall on or about the heavy black line.

Insulation-Controlled Regime — Comprising the points to the left of the heavy black line, and which are asymptotic towards E_{min}.

Surface-Controlled Regime — Comprising the points to the right of the heavy black line, and which asymptotic towards E_{max}.

Fig. 2. Correlation of predicted error, E, with dimensionless parameters (for surface mounted HFS without edge guards).

Hence from equation (1c)

$$H = \frac{(0.042)^2}{1.50 \times 0.07}\sqrt{\frac{0.037.(0.01 \text{ to } 0.05).0.07}{(0.05)^2}}$$

$$= 1.8 \times 10^{-3} \text{ to } 4.0 \times 10^{-3}$$

from equation (1)

$$E = 12\text{–}14\%$$

if in the power-law regime.

Note that

$$E_{min} = \frac{0.042}{(0.042 + 1.5)} \rightarrow 2.7\%$$

$$E_{max} = \frac{0.042}{(0.042 + 0.07)} \rightarrow 37.5\%.$$

Since E does not approach either E_{min} or E_{max}, we conclude that the HFS will operate in the power-law regime, with a measurement error of 12–14%. Darnell's reported error for this case was 16%.

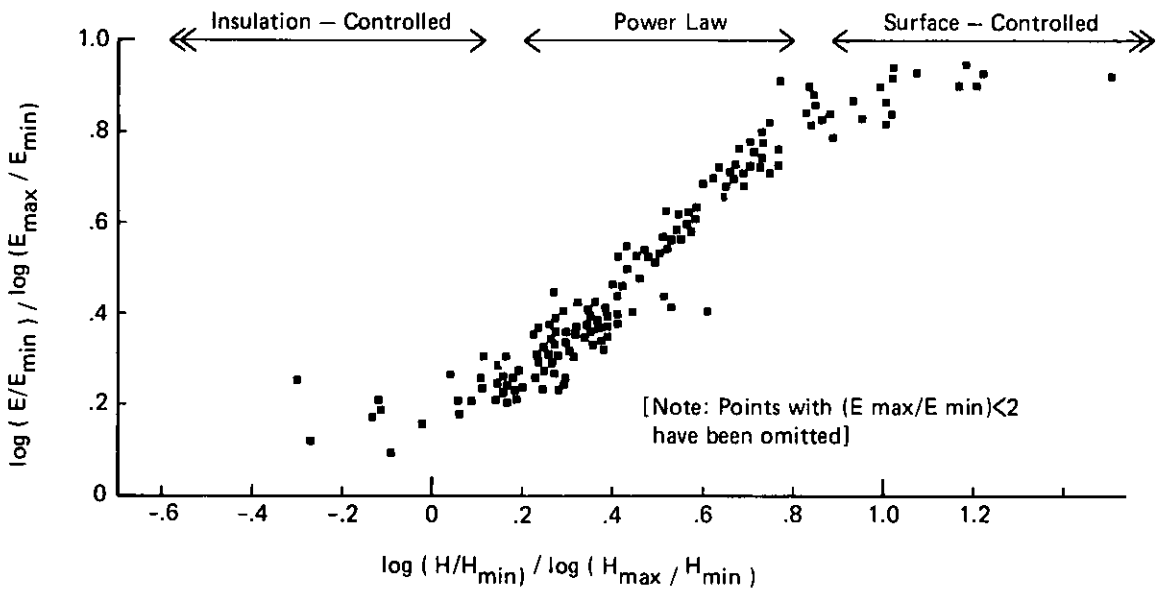

Fig. 3. A normalised version of Fig. 2.

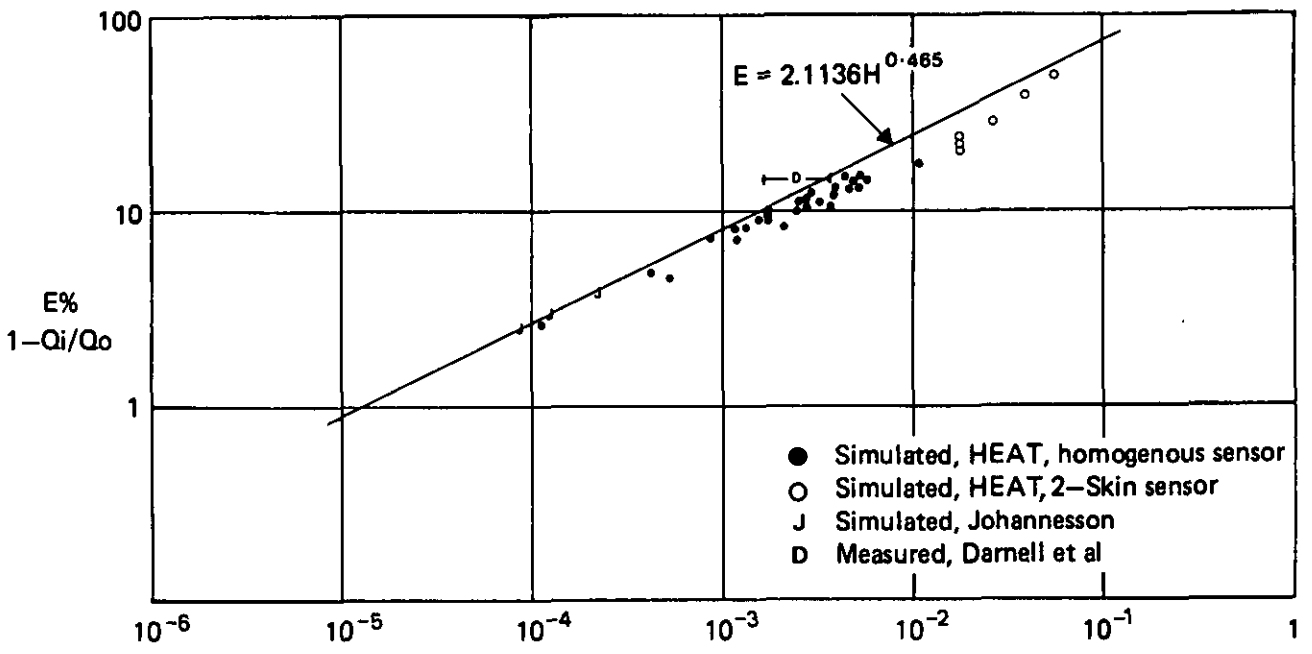

$$H = \frac{R_m}{R_t} \cdot \frac{R_m}{R_s}\sqrt{\frac{ktR_s}{L^2}}$$

(a) Predicted or observed error v H for cases in the POWER-LAW regime

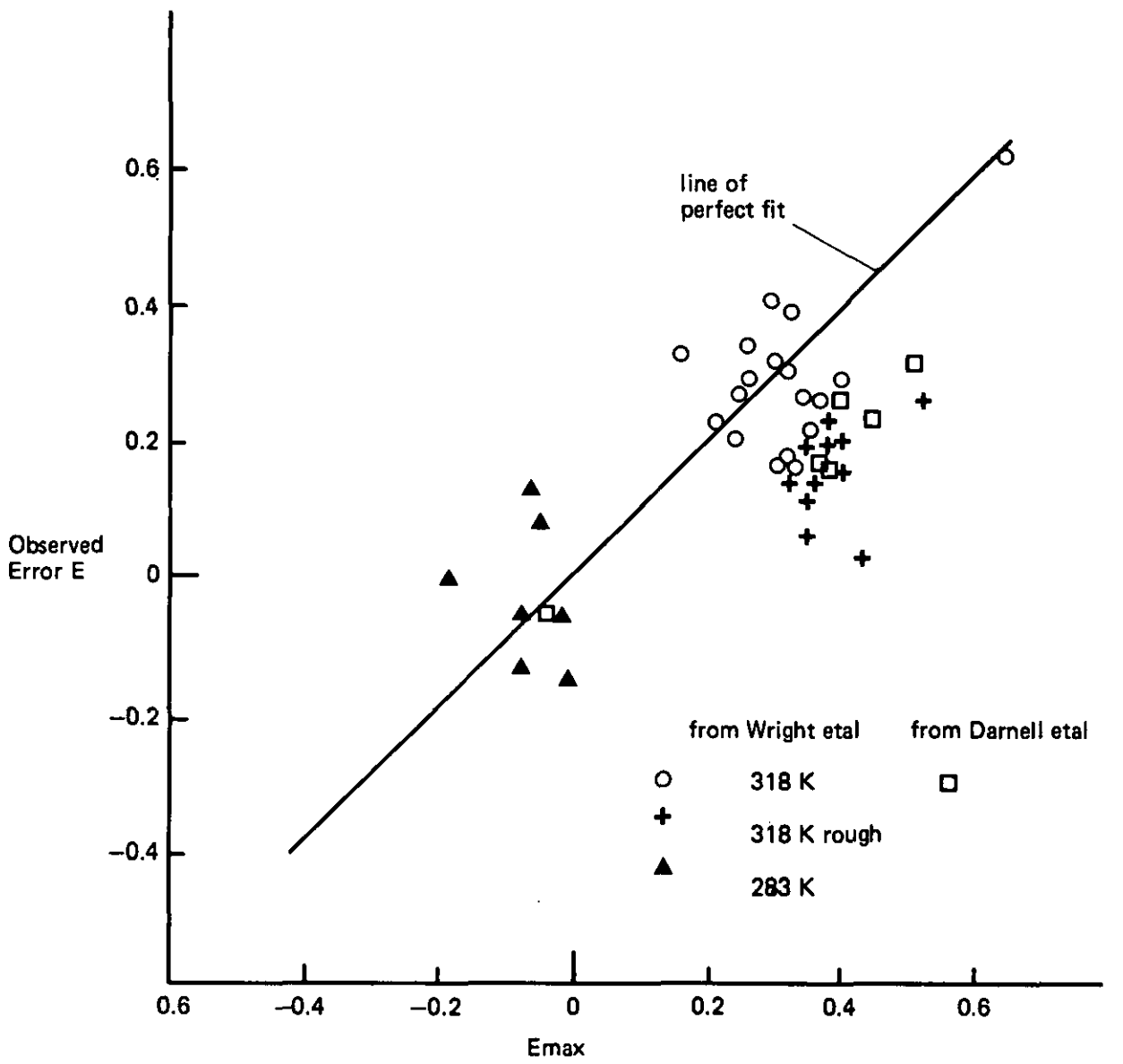

(b) Observed error v Emax for cases in the SURFACE-CONTROLLED regime

Fig. 4. Comparison of predicted error, E, with data from independent sources.

4.2. *Comparison of independent data with parametric model*

Having established a model, we now endeavour to test its validity against data from independent sources.

Firstly, the predictions from an entirely different computer simulation program HEAT were used to test whether there were any important errors in HFSIM. These comparisons [see Fig. 4(a)] show that two completely independent programs give closely similar results, and that closely similar results are also obtained with two radically different designs of HFS (one made from two parallel aluminium plates, the other from a homogenous wafer of material). Johannesson's simulations referring to various substrate conductivities are also illustrated in Fig. 4(a).

Secondly, we consider the reported experimental data available. Johannesson [9] reports on the effect of surface resistance, and shows measured 'error' increasing with local air velocity but reaching a limit at high velocities, in contrast to his own 'predicted error' which continued to

rise with velocity. This feature of his data fits comfortably with the prediction of equations (1). Johannesson's tests did however include an air space between the HFS and the substrate, and some wind penetration under the HFS was possible. Johannesson interpreted the whole of the error change as due to wind penetration. However equations (1) predict about half the error observed by Johannesson, even without invoking wind penetration.

Wright *et al.* [19] presented very detailed laboratory measurements, made with an HFS mounted on blackened copper or aluminium base plates. This enabled them to determine contact resistances and surface heat transfer coefficients, but it does not provide particularly suitable data against which equations (1) can be tested. On such a substrate, the measurement error would be operating in the surface-controlled regime, and depend only on sensor, contact and surface resistances. It is possible to express their data in a form allowing observed error E to be compared with E_{max}. See Fig. 4(b). The fit is reasonably good, but with considerable scatter, as might be expected given that the temperature measurement resolution was only about 0.5°C.

Darnell *et al.* [20] also presented very detailed laboratory measurements in which HFSs were placed over typical building material substrates. Most of their results were also in the surface-controlled regime, but one case (HFS over 50-mm expanded polystyrene) fell within the power-law zone. Darnell's data is particularly significant for the deliberate manipulation of surface emittances of sensor and surrounding substrate. Such variation is important in practice, and it can be also coped with by the predictive methods proposed here, so Darnell's data should provide a valuable test. However, although commenting that their data showed a different (usually higher) surface resistance over the HFS than elsewhere, Darnell did not provide information on the differences. When Darnell's data is overlayed on Figs 4(a) and (b), there is excellent agreement in the one case in the power-law zone. In all other cases the agreement is less good, which may be expected because of the high sensitivity to surface resistance when the surface-controlled regime is approached.

4.3. *Analytic treatment*

The general case of an insulating patch over a conducting base has not been solved and has been described as intractable. However Weir [22] has generated an analytic solution to the problem of a circular HFS over a two-layer substrate. Equations (2) are applicable approximations derived from this solution.

This is:

$$E \cong 1-\alpha\beta^*/\{\beta[\alpha^*+2(\beta^*-\alpha^*)J_{00}(\beta^*)]\} \quad \text{for} \quad \beta^* > 1$$
$$E \cong 1-\alpha[1+8(\beta^*-\alpha^*)/3\pi]/\beta \quad \text{for} \quad \beta^* < 1 \qquad (2)$$

where

$$\alpha = L/(2k_1R_1), \qquad \beta = L/(2k_1R_2)$$
$$\alpha^* = \frac{G(1)[1+\alpha G(0)]}{[G(0)-G(1)]}, \qquad \beta^* = \frac{G(1)[1+\beta G(0)]}{[G(0)-G(1)]}$$
$$G(0) = (2k_1/L)(Z_1+Z_2)$$

$$G(1) = \frac{k_1 \tanh(2t_2/L)+k_2 \tanh(2t_1/L)}{k_2+k_1 \tanh(2t_2/L)\tanh(2t_1/L)}$$

t_1, t_2 = layer thickness
k_1, k_2 = layer conductivity
Z_1, Z_2 = layer resistance ($= t/k$)

} 1 = surface layer; 2 = deeper layer

L = HFS diameter

R_1 = total surface resistance at HFS (sensor + contact + HFS surface resist)

R_2 = surface resistance for surrounding surface

$$J_{00}(\beta) \cong \frac{1}{\pi\beta}(\ln\beta+0.657).$$

The fit between equations (1) and (2) is illustrated in Fig. 5. It may be noted that there is a general agreement between the two predictions, but not necessarily a close agreement in individual cases. This lack is attributed to the fact that the $G(0)$ and $G(1)$ functions are themselves approximations, but of similar size, and a $[G(1)-G(0)]$ term appears in the denominator of α^* and β^*. No explanation is offered on why the predictions from Weir's formulae are consistently low compared to simulated results. Improvements to the reliability of the above estimates are possible.

5. PRACTICAL CONSEQUENCES FOR SURFACE-MOUNTED HFS

The relations in equations (1) and (2) carry some important messages regarding the design and use of HFSs. Some of these messages are already widely accepted but others are novel. They are discussed below in four groups.

5.1. *Calibration*

The use of the guarded hotplate for calibration has been widely advocated. The practical difficulties of edge guarding an unknown HFS, and the fundamental difficulty posed by the fact that real HFSs have edges of finite thickness, have already been described. On the latter point it may be noted that the ratio of edge/face areas of HFSs described in the literature varies between 1.5 and 71%. In some commercial sensors the edge/face area ratio exceeds 100%. Given the variety of ways in which HFSs can be constructed and applied, it is difficult to see how the in-service HFS edge heat losses might in general affect the apparent calibration constant obtained from a guarded hotplate. Simple calculations indicate an adjustment pro-rata to the edge/face area ratio.

For this reason, several other calibration methods which allow edge losses from the HFS have been used. Haupin and Luffy [13] used a heater plate with edge guarding, a rather elegant procedure but one which would require new equipment for every different size of HFS calibrated. Trethowen [21] used a heater-foil method which can accommodate a very wide range of HFS sizes. That method has been found to be excellent for what may be termed 'engineering grade' calibration. There are some as-yet unsolved difficulties which limit its usefulness for 'laboratory grade' calibration.

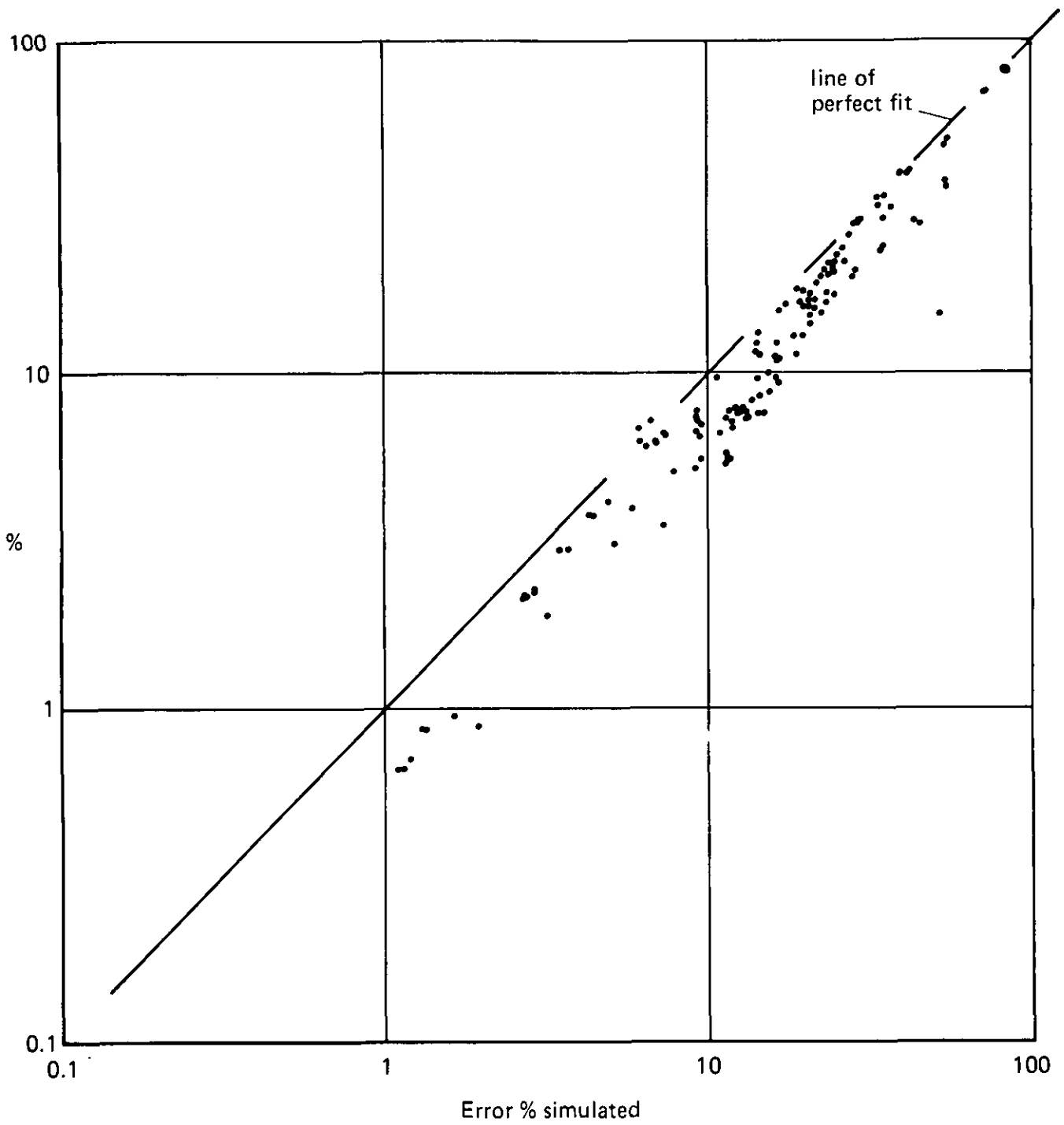

Fig. 5. Comparison of error predicted by equation (2) vs Tables 1 and 2.

5.2. *Surface heat transfer conditions*

Equation (1) indicates that the measurement error is fairly insensitive to surface heat transfer resistance, except in the surface-controlled regime. When HFSs are used in indoor building applications, the latter condition is usually encountered only with small sensors. This suggests that for consistent performance, large HFSs should be preferred [see equation (1) to determine the meaning of 'small' and 'large']. This is a new suggestion which does not appear in previous literature.

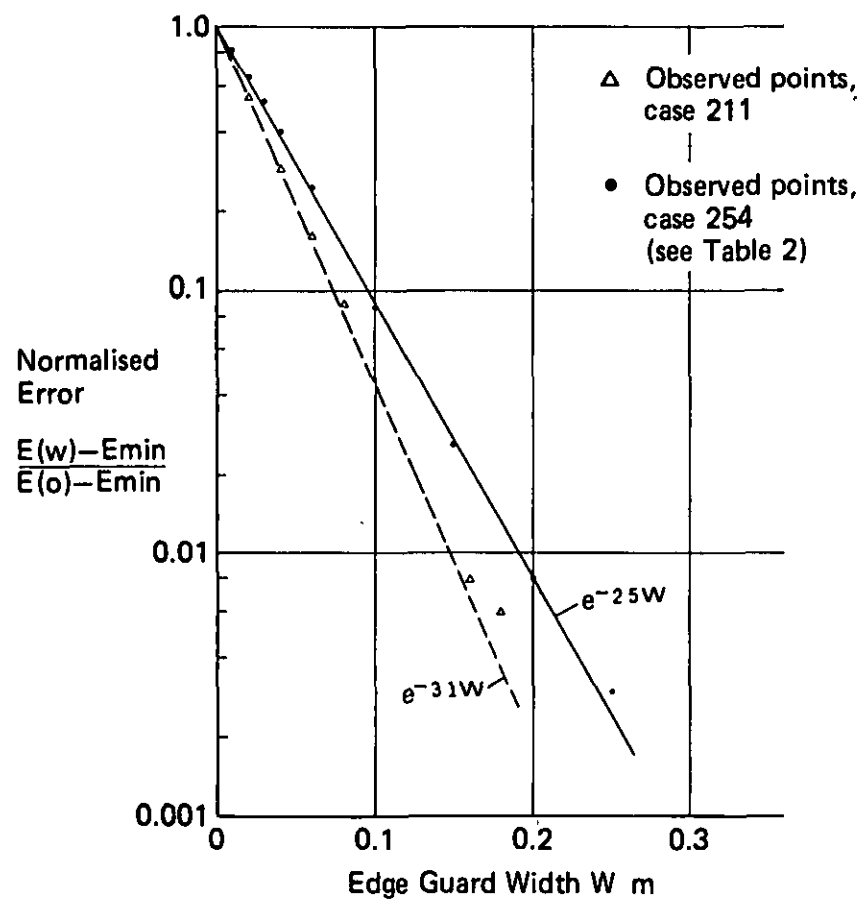

Fig. 6. Comparison of predicted error with edge guard width.

A number of authors have commented on real or possible differences between the surface heat transfer conditions over the HFS, and over the remaining undisturbed surface. Some authors (e.g. [14, 15–17, 19, 20]) have placed major emphasis on the surface heat transfer conditions. Others, (e.g. [9]) have reported measurements which indicate that considerable changes in surface heat transfer coefficient can take place without large effects on the error. Figure 2 shows how this apparent contradiction can arise, and that there are identifiable conditions which lead to either low or acute sensitivity to surface heat transfer coefficients.

In the event that the surface heat transfer coefficient over the HFS is different to that elsewhere, this is accommodated using (1d), to adjust the effective sensor resistance R_m. The effects are explored in Fig. 7 for typical cases, and this illustrates that the consequences of surface heat transfer coefficient variations are small in the insulation-controlled regime and in the power-law regime, but become acute in the surface-controlled regime.

The effective sensor resistance R_m can even become zero

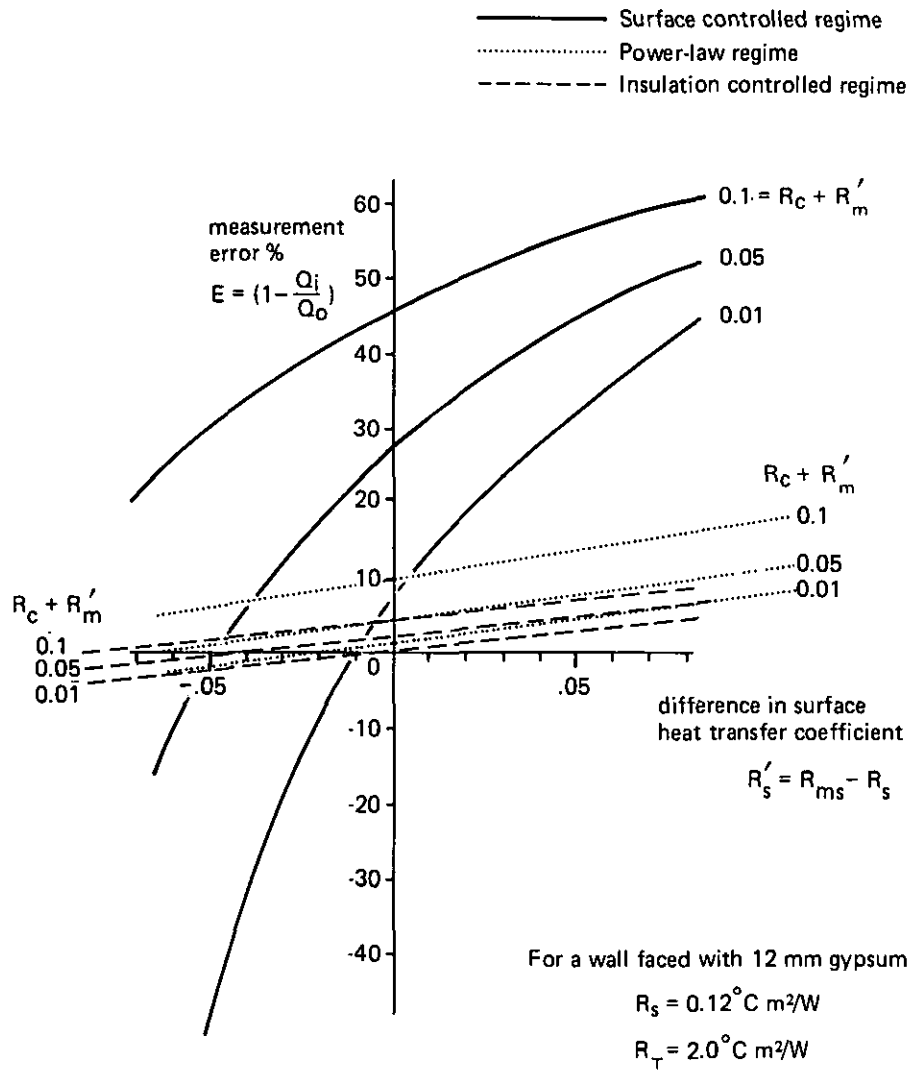

Fig. 7. Sensitivity of error, E, to differences in surface heat transfer coefficient.

or negative, and this has occurred in Darnell *et al.*'s [20] and Wright *et al.*'s [19] results.

The condition where environmental radiant and convective surrounds differ has not been explored here. Further transformations would account for such differences.

5.3. *HFS design*

Whilst it has long been recognised that small values of sensor and contact resistance are desirable to minimise measurement error, other aspects of HFS design appear to have been overlooked.

The first such feature is the advantage of a large size (e.g. diameter) of HFS. This not only reduces the measurement error, but is also likely (as discussed in Section 4.2) to move the operating condition of the sensor into a state where it is insensitive to changes in the surface heat transfer coefficients.

It should also be noted that in equations (1) and (2), the contact resistance R_c between sensor and substrate has no special significance. The measurement error is a function of the sum of sensor and contact resistances. If one is relying on a very low value of sensor resistance for the required accuracy, then of course failure to achieve a low contact resistance would be of major concern. But if a higher sensor resistance can be used (perhaps by choosing a large sensor) then variations in the contact resistance may become unimportant.

Mention has already been made of the possible effects of the edge surfaces of HFSs. High ratios of edge/face area tend to occur with small sensors. One may note that in a sensor only 2.5 mm thick, the edge area is equal to the face area for a 10 mm square sensor.

Thus a picture emerges that large (diameter) HFSs are not only intrinsically more accurate, they are also less affected by practical variations in contact and surface resistances.

One may also note that thermopile-type HFSs can be affected by lateral temperature differences over the area covered by the sensor. If such temperature differences are encountered, their effect can readily swamp the signal generated by normal heat flow. This sensitivity can be readily avoided by adopting a suitable wiring pattern. All the early designs of HFS avoided this problem, but Huebscher [5] is the only author to have specifically identified it. It must be regarded as a serious deficiency of all HFSs in which a thermopile coils in one direction only.

5.4. *Edge guarding*

The information in equations (1) and (2), and Fig. 4 refer to sensors without edge guarding. The effect of edge guarding on measurement error has also been examined by finite-difference simulation, with the conclusion that the width of edge guard required is a strong function of the ratio E/E_{min}. The required edge guard width reduces as the total structure resistance increases, and as the sub-

strate conductivity or thickness reduces, but these effects are much weaker.

The effect of various degrees of edge guarding has been examined for some 40 cases in Table 2. Empirical fitting showed that virtually all of these cases followed equation (3) with remarkable agreement—see Fig. 6. The value of the exponent a varies for the different cases with a mean of 31, standard deviation of 9. It was observed that the larger values of exponent a were associated with cases in the insulation-controlled regime, whilst smaller values were associated with the surface-controlled regime.

$$\frac{E(w)-E_{\min}}{E(0)-E_{\min}} = e^{-aw} \tag{3}$$

where

w = edge guard width, m
$E(w)$ = error at edge guard width W
$E(0)$ = error with zero edge guarding
a = fitted constant (see above), typically 30.

This indicates that for building applications, edge guard widths of 50–200 mm will be required to ensure that the error $E(w)$ is very little greater than the minimum error $E_{\min}$. Sensors with smaller edge guards than this should be regarded as being partially edge guarded.

5.5. *Manufacturer's data*

The manufacturers of HFSs face many difficulties. This investigation suggests at least a schedule of properties that manufacturers should be able to supply.

Calibration constant (this should be the 'true' calibration, relative to heat flux through sensor, at a range of temperatures) with accuracy tolerances
Physical dimensions
Physical exposure limitations
Surface emittance
Details of any internal edge guarding—or size of active sensing area
Sensitivity to lateral temperature differences (e.g. μV per °C edge/edge temperature difference).

Unless a sensor is being sold in a proprietary rig for specific limited uses, manufacturers should resolutely refrain from any claims of in-service accuracy.

CONCLUSIONS

The following conclusions are drawn in this paper, in regard to surface-mounted heat flux sensors.

1. The measurement error is a function of the measured structure as well as of the sensor and can not be considered in isolation from the structure and the surface conditions.
2. Measurement errors can be quantified with moderate accuracy over a wide range of operating conditions. Two methods of prediction are offered. There are absolute upper and lower bounds to the measurement error, and three operating regimes referred to as the insulation-controlled, power-law and surface-controlled regimes, respectively.
3. Contact resistances and differences between surface resistance of HFSs and of remaining surface do not always have to be eliminated, just known. For sensors operating in the power-law or insulation-controlled regimes, these resistances are of minor significance, but for sensors working in the surface-controlled regime the sensitivity is acute.
4. Measurement errors can be reduced by:

   Increasing—size (diameter or edge length) of sensor
   —surface resistance
   —thermal resistance of wall under test
   —edge guarding
   Decreasing—sensor + contact resistance
   —conductivity and thickness of surface layer of substrate.

5. Large size (diameter or edge length) of HFS is predicted to provide many advantages in reducing measurement error, and also in stabilising these errors (e.g. against fluctuations in surface resistance from varying air velocity).
6. The issue of how HFSs for surface mounting should be calibrated remains open. The use of 'true' rather than 'corrected' calibration constants is advocated, and there is a problem of edge area of HFSs.
7. Makers of HFSs should note a need to avoid and/or declare the sensitivity of their devices to lateral temperature gradients; to minimise the ratio of edge/face areas; to note the advantages of large sensors; and to declare details of edge guarding, sensor resistance, emittance and calibration procedure.

REFERENCES

1. F. C. Houghten, A study in heat transmission with special reference to building materials, *ASHVE Trans.*, New York paper 619, pp. 81–102 (1922).
2. P. Nicholls, Measuring heat transmission in building structures and a heat transmission meter, *ASHVE Trans.*, New York paper 685, pp. 65–103 (1924).
3. P. Nicholls, Practical applications of the heat flow meter, *ASHVE Trans.*, Kansas paper 701, pp. 289–299 (1924).
4. F. C. Houghten, C. Gutberlet and C. G. F. Zobel, Additional coefficients of heat transfer as measured under natural weather conditions, *ASHVE Trans.*, Chicago paper 824, pp. 151–164 (1929).
5. R. G. Huebscher, L. F. Schutrum and G. V. Parmalee, A low inertia low-resistance heat flow meter, *ASHVE Trans.*, Spring Lake paper 1453, pp. 275–286 (1952).
6. J. R. Philip, The theory of heat flux meters, *J. geophys. Res.* **66**, 571–579 (1961).
7. P. Schwerdtfeger, The measurement of heat flow in the ground and the theory of heat flux meters, Cold Regions Research and Engineering Laboratory, U.S. Army, NH (1970).
8. J. de Jong and L. Marquenie, Heat flowmeters and their applications, *Instrum. Pract.* 45–51 (January 1962).
9. G. Johannesson, Heat flow measurements, thermo-electrical meters, functions principles and sources of

error, Division of Building Technology, Lund Institute of Technology, Report TVBH-3003 (U.S.A. Cold Regions Research and Engineering Laboratory Draft Translation) (1979).
10. C. L. Heard and I. C. Ward, The design and use of low-cost heat flux plates for the measurement of building heat transfer rates, *Bldg Envir.* **17**, 229–233 (1982).
11. R. A. Grot, *In-situ* measurements of building envelope thermal properties, *Proc. Building Thermal Mass Seminar*, DOE/ORNL, pp. 313–319 (June 1982).
12. P. E. Condon and W. L. Carroll, Measurement and analysis of in-situ dynamic thermal performance of building envelopes using heat flow meter arrays, *Proc. ASHRAE/DOE-ORNL Conference on Thermal Performance of the Exterior Envelopes of Buildings.* ASHRAE SP 28, pp. 740–750 (1979).
13. W. E. Haupin and J. W. Luffy, Construction and calibration of rugged heat flow meters, 106*th Annual Meeting of AIME*, Atlanta GA, pp. 125–132 (1977).
14. S. N. Flanders, Time constraints on measuring building *R*-values, Cold Regions Research and Engineering Laboratories, U.S. Army, NH, CRREL Report 80–15 (1980).
15. S. N. Flanders, *In-situ* measurement of masonry wall thermal resistance, *ASHRAE Trans.* **88**, 677–688 (1982).
16. S. N. Flanders and S. J. Marshall, Towards *in-situ* building *R*-value measurement, Cold Regions Research and Engineering Laboratory, Report 84-1, NH (1984).
17. S. N. Flanders, Confidence in heat flux transducer measurements, *ASHRAE Trans.* **91**, 515–531 (January 1985).
18. F. De Ponte and W. Maccato, The calibration of heat flow meters. *Thermal Insulation Performance*, ASTM STP 718, pp. 237–254. American Society for Testing and Materials, New York (1980).
19. R. E. Wright, A. G. Kantsios and W. C. Henley, Effect of mounting on the performance of surface heat flow meters used to evaluate building heat losses. *Thermal Insulation, Materials and Systems for Energy Conservation in the '80's*, pp. 293–317, ASTM STP 789. American Society for Testing and Materials, New York (1983).
20. A. J. Darnell, L. R. McCoy and M. B. Ingle, Evaluation of factors affecting heat flux sensors, Energy Technology Engineering Centre, Rockwell International. Available NTIS CONF-830, pp. 622–25, (1983).
21. H. A. Trethowen, Engineering application of heat flux sensors in buildings—the sensor and its behaviour, Building Applications of Heat Flux Transducers, ASTM STP885, pp. 9–22. American Society for Testing and Materials, New York (1983).
22. G. J. Weir, Heat flux sensors, *J. Aust. Math. Soc.* **B27**, 281–294 (1986).

Measurement errors with s
urface-mounted heat flux

BUILDING RESEARCH ASSOCIATION OF NEW ZEALAND INC.
HEAD OFFICE AND LIBRARY, MOONSHINE ROAD, JUDGEFORD.

The Building Research Association of New Zealand is an industry-backed, independent research and testing organisation set up to acquire, apply and distribute knowledge about building which will benefit the industry and through it the community at large.

Postal Address: BRANZ, Private Bag, Porirua

ISSN 0111–7459